DOI: 10.1021/cg100609h

CRYSTAL GROWTH & DESIGN Article

2010, Vol. 10
4023–4029

Ternary Solubility Phase Diagrams of Mandelic Acid and *N*-Methylephedrine in Chiral Solvents with Different Carbon Chain Lengths

Samuel Kofi Tulashie,[†] Heike Lorenz,*[,†] Chandrakant Ramkrishna Malwade,[‡] and Andreas Seidel-Morgenstern[†,‡]

[†]*Max Planck Institute for Dynamics of Complex Technical Systems, Magdeburg, Germany, and* [‡]*Otto von Guericke University, Magdeburg, Germany*

Received May 7, 2010; Revised Manuscript Received June 30, 2010

ABSTRACT: Ternary solubility phase diagrams of mandelic acid and *N*-methylephedrine species in chiral solvents, (*S*)-methyl lactate, (*S*)-propyl lactate, and (*S*)-butyl lactate, have been determined. Solubility measurements were performed for enantiomeric compositions ranging from 50:50 mixtures to the pure enantiomers and temperatures ranging from 0 to 35 °C for mandelic acid and from 0 to 25 °C for *N*-methylephedrine, respectively. The ternary solubility phase diagrams of mandelic acid and *N*-methylephedrine showed symmetric behavior. It became obvious that increasing chain length of chiral solvents, i.e. from (*S*)-methyl lactate to (*S*)-butyl lactate, resulted in decreasing solubility. ^{1}HNMR and Raman spectroscopy have been applied to characterize the solute-solvent interaction in the liquid phase for mandelic acid system. Molecular modeling calculations were performed for mandelic acid to get a deeper understanding of the solute−solvent interactions. The effect of the solvent on the shape of the solubility isotherms is discussed by determining the relative solubility ratios (α_{mol}-values) just for *N*-methylephedrine.

Introduction

Enantioseparation is of great importance to the pharmaceutical industry due to the fact that more than 50% of the active pharmaceutical ingredients produced are chiral in nature.[1,2] Many of the drugs currently used in practice are 50:50 mixtures of enantiomers (racemates). For some therapeutics, single-enantiomer formulations can provide greater selectivities for their biological targets, improved therapeutic indices, and better pharmacokinetics than a mixture of enantiomers. Also, sometimes the presence of the biologically inactive enantiomer shows adverse effects, therefore reducing the efficiency of the drug.[3] The demand for single enantiomers is increasing more, especially after the Thalidomide tragedy, due to the stringent restrictions set by FDA over the use of drugs in racemate form.[4]

Due to identical behavior of the enantiomers in most chemical and physical properties, enantiomers are difficult to separate. Pasteur successfully separated enantiomers of sodium ammonium tartrate, as they formed crystals which were mirror images of each other.[5] However, the feature of enantiomers forming mirror shaped crystals which was exploited effectively by Pasteur is rather limited to a few cases. New enantioseparation techniques started developing after Roozeboom[6] identified the three basic racemate types based on their melting point phase diagrams, as conglomerate, racemic compound, and pseudoracemate. Among these three types of racemates, conglomerates are far easier to resolve than racemic compounds.[7] Unfortunately, conglomerates account for only 5−10% of all chiral compounds, thus racemic compounds form the majority portion of cases.[8] Single enantiomers can be produced either by means of asymmetric synthesis or by separating the racemic mixtures. In recent years, considerable progress has been achieved in the field of enantioselective catalysis.[9,10] However, it is still short of providing economical selective reactions leading to a variety of enantiomers. Hence, there is a high demand for more generally applicable and cheap separation processes. The well-known techniques employed to resolve racemic mixtures into enantiomers are preparative chromatography,[11] crystallization via formation of diastereomeric salts,[12] preferential crystallization,[13] and enzymatic resolutions.[14] Among these separation techniques, preferential crystallization is emerging as one of the methods of choice for enantioseparation due to economical reasons.[15] Designing such a process requires detailed information about the solid−liquid equilibria, its temperature dependency, and the solvent system used. For example, while working with materials having a steep solubility curve, it is common to use cooling type crystallizers, whereas, with the materials having a moderate slope of the solubility curve, evaporative cooling, surface cooling, or constant temperature evaporation is preferred.[16] To evaluate the effect of decreased and increased chain length in the solvent molecule on the solubility of mandelic acid and *N*-methylephedrine, more systematic experimental work is required and is the focus of this study.

The present work is concerned with the determination and analysis of the ternary solubility phase diagrams of mandelic acid (a racemic compound-forming system) and *N*-methylephedrine (a conglomerate-forming system) in three chiral solvents: (*S*)-methyl lactate, (*S*)-propyl lactate, and (*S*)-butyl lactate at different temperatures. In previous work, the solubilities of mandelic acid and *N*-methylephedrine in the chiral solvent (*S*)-ethyl lactate have been reported.[17,18] However, to verify the effect of decreased and increased chain length in the solvent molecule on the solubility of mandelic acid and *N*-methylephedrine, the chiral solvents (*S*)-methyl lactate, (*S*)-propyl lactate, and (*S*)-butyl lactate were now included in the studies.

In the following, first the ternary solubility phase diagrams of mandelic acid and *N*-methylephedrine as a function of temperature and as a function of different chiral solvent chain lengths will be discussed. Afterward, on example of mandelic acid, the underlying solute−solvent interactions in solution will be evaluated by means of Raman and ^{1}H NMR measurements and molecular modeling calculations. Further, the relative

*To whom correspondence should be addressed. Present address: Heike Lorenz, Max Planck Institute for Dynamics of Complex Technical Systems, Sandtorstrasse 1, D-39106 Magdeburg, Germany. Telephone: (0049) 391 6110 293. Fax: (0049) 391 6110 524. E-mail: lorenz@mpi-magdeburg.mpg.de.

Published on Web 08/05/2010

solubility ratios (α_{mol}-values) derived from the solubility isotherms for the *N*-methylephedrine chiral system in all solvents are discussed in relation to enantioselective process design.

Experimental Section

Chemicals. Mandelic acid (enantiopure and racemic) and *N*-methylephedrine (enantiopure) obtained from Aldrich or Merck with purities ≥99% were used. The chiral solvents (*S*)-(−)-methyl lactate, (*S*)-(−)-propyl lactate, and (*S*)-(−)-butyl lactate were obtained from PURAC Netherlands with purities ≥97%. For the ^{1}H NMR experiments, methanol-d_4 obtained from Deutero GmbH with purity ≥99.8% was used.

Solubility Measurements. An isothermal measurement technique was used to measure the solubilities of mandelic acid at the temperatures 0, 5, 15, 25, and 35 °C and of *N*-methylephedrine at the temperatures 0, 5, 15, and 25 °C in the chiral solvents considered for the study. A 5 mL solute−solvent mixture with a large excess of solid phase was prepared and placed into a 10 mL sealed glass vessel with a magnetic stirrer. The solvent−solute mixture was then gently heated under constant stirring of 400 rpm to achieve a homogeneous state and then cooled down under constant stirring to the desired saturation temperature. Afterward, liquid samples were isolated by filtration through a glass filter (pore size 10 μm). Equilibrated crystallized materials were analyzed with X-ray powder diffraction (XRPD), while the clear solution obtained after filtration was analyzed with a chiral HPLC to determine the composition as well as concentration of the solution. The experiments lasted for 24 h to ensure equilibration. Measurements were repeated at least two times.

(**a**) **Liquid Phase Analysis.** The liquid samples collected from the solubility experiments were diluted with isopropanol. The concentration of the solution and the enantiomeric composition were determined with chiral HPLC:

An Agilent HP 1100 unit with a Chiracel OD-H column (Astec, 250 mm × 4.6 mm/5 μm) for mandelic acid analyses and a Eurocel OD column (Knauer, 250 mm × 4.6 mm/5 μm) for *N*-methyl ephedrine analyses was employed. The column temperature was 25 °C, and the flow rate was 1 mL/min. A UV diode array detector was applied for peak detection at a wavelength of 254 nm. The eluent fractions by volume (φ) were as follows:

(1) Mandelic acid in chiral solvents used: φ (*n*-hexane) = 0.84, φ (isopropanol) = 0.16, and φ (trifluoroacetic acid) = 0.001.
(2) *N*-Methylephedrine in chiral solvents used: φ (*n*-hexane) = 0.85, φ (isopropanol) = 0.15, and φ (diethylamine) = 0.001.

(**b**) **Solid Phase Analysis.** These measurements were undertaken to identify the type of species present and also to check for differing solid state forms (solvates and/or polymorphs). The crystalline materials were characterized on a PANalytical X'Pert Pro diffractometer with Cu Kα radiation at 40 mA and 40 kV. The scanned 2θ region was 3° to 40° with a step size of 0.017° and a counting time of 50 s per step.

Solute−Solvent Interactions in Liquid State for Mandelic Acid. (a) ^{1}H NMR Measurements. ^{1}H NMR spectra were recorded on a Bruker AVANCE 600 spectrometer at 600.13 MHz. The AVANCE 600 is fitted with a 5 mm PTXI-1H-13C/15N/2H probe head with *z*-gradients. The samples were measured in methanol-d_4 deuterated solvent as an internal lock. Spectra were recorded at T = 293 K with a pulse width of 7.8 μs for a 90° pulse. The ^{1}H NMR chemical shifts (δ) were reported in parts per million downfield from TMS (internal).

The samples were prepared in NMR tubes as follows:

Test samples:

(1) (*S*)-mandelic acid (10 mM) + (*S*)-methyl lactate (50 mM) + CD_3OD (600 μL)
(2) (*R*)-mandelic acid (10 mM) + (*S*)-methyl lactate (50 mM) + CD3OD (600 μL)

Reference sample:

(*R*)-mandelic acid (10 mM) + CD_3OD (600 μL)

This procedure was repeated for the other chiral solvents studied.

(**b**) **Raman Measurements.** Raman spectra were measured using a MultiRAM spectrometer from BRUKER Optik GmbH. The system uses a laser beam of 1064 nm operating at 300 mW. The analyses were carried out for liquid phase samples at ambient temperature. The samples were scanned for a period of 10 s; the resolution was 4 cm^{-1}. Liquid phase samples of (*S*)- and (*R*)-mandelic acid in (*S*)-methyl lactate, (*S*)-propyl lactate, and (*S*)-butyl lactate at a concentration of 8 wt % were studied.

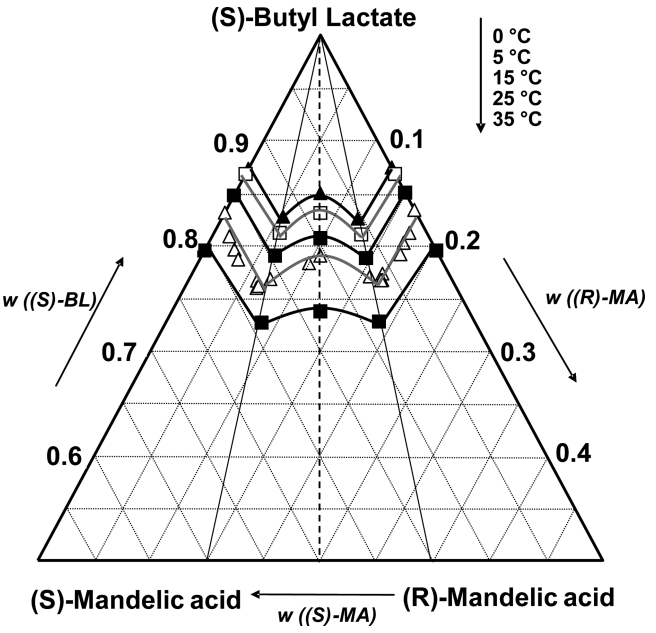

Figure 1. Ternary solubility phase diagram of mandelic acid in the chiral solvent (*S*)-butyl lactate at temperatures ranging from 0 to 35 °C (BL, butyl lactate; MA, mandelic acid). The isothermal lines have been added as a visualization aid, and only the marked points show measured data.

(**c**) **Molecular Modeling.** The enthalpy of formation calculations were performed by employing the VAMP module in MATERIALS STUDIO from the software package Accelrys Materials Studio 4.3,[19] which uses a general purpose semiempirical quantum mechanics program for the study of structural optimization as a preliminary approach to calculate the enthalpy of formation. The VAMP module is used together with Austin model 1 (AM1), which gives a good estimation for hydrogen bonding calculations.[20,21]

Results and Discussion

Ternary Solubility Phase Diagrams. Figures 1 and 2 exemplarily show the determined ternary solubility phase diagrams of (*S*)-butyl lactate and the two enantiomers of mandelic acid and *N*-methylephedrine at different temperatures, respectively. Both figures show the typical behavior of a racemic compound and a conglomerate forming system, respectively. The solubility isotherms are determined at temperatures ranging from 0 to 35 °C for mandelic acid and from 0 to 25 °C for *N*-methylephedrine. The phase diagrams for both mandelic acid and *N*-methylephedrine show symmetric behavior in the temperature range studied. The eutectic compositions of the mandelic acid enantiomers remain unchanged, as also observed in water and the binary melting point phase diagram at 31/69 or 69/31, respectively.[13,22,23]

For both mandelic acid and *N*-methylephedrine, solubility increases with increase in temperature; in fact, the increment is linear. It became evident that the solubility of the racemic species exceeds that of the corresponding enantiomers in both systems. In most cases, the solubility of solids increases with increase in temperature, with few exceptions, where solubility is almost independent of temperature (e.g., sodium chloride[16]) and examples of retrograde solubility. The same trend applies to the solubility of mandelic acid and *N*-methylephedrine in the other solvents used; that is, the solubility increases with increasing

temperature within the measured temperature ranges. Moreover, varied temperature had no effect on the eutectic composition of the enantiomers in the phase diagram.

Figure 3 exemplarily depicts experimental patterns of *N*-methylephedrine obtained during solubility measurements in (*S*)-butyl lactate as solvent at 25 °C. *N*-Methylephedrine, being a conglomerate-forming system (Figure 2), must show identical reflexes for enantiomers, the racemic mixture, and thus also all mixtures of them. From Figure 3, it is clear that various enantiomeric compositions of *N*-methylephedrine exactly imitate the reflexes of the references, confirming the absence of any new phases such as solvates or a polymorph under the conditions used. Hence, the solubilities measured all refer to the known solid phases in the system. The same applies to the other solvents and the mandelic acid cases too. Although for racemic mandelic acid a further metastable modification occurs,[22] in the chiral solvents used here, just the stable modification was found. Additionally, no solvates are formed.

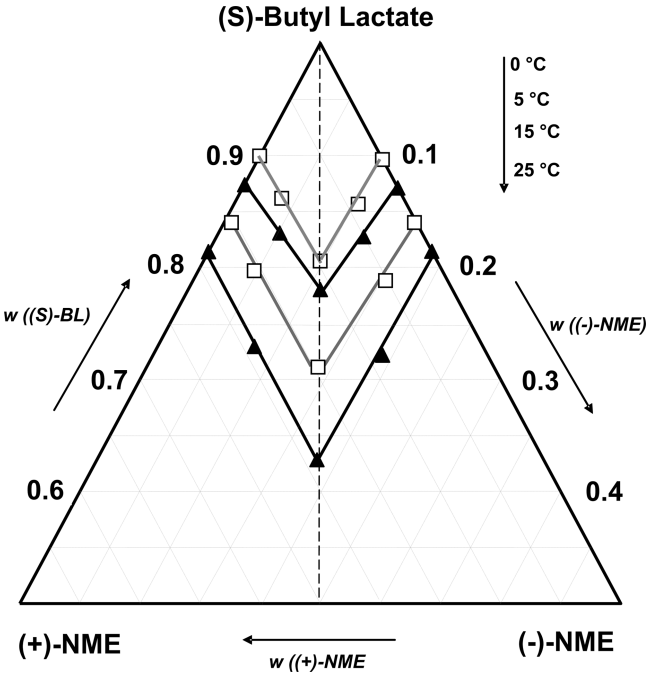

Figure 2. Ternary solubility phase diagram of *N*-methylephedrine in chiral solvent (*S*)-butyl lactate at temperatures ranging from 0 °C to 25 °C. (NME, *N*-methylephedrine). The isothermal lines have been added as a visualization aid, and only the marked points show measured data.

Effect of Chain Length of Solvent Molecules on Solubility. Figures 4 and 5 show the derived ternary solubility phase diagrams of mandelic acid and *N*-methylephedrine in the solvents (*S*)-methyl lactate, (*S*)-ethyl lactate, (*S*)-propyl lactate, and (*S*)-butyl lactate at 25 °C, respectively. Solubility data for mandelic acid and *N*-methylephedrine enantiomers in (*S*)-ethyl lactate have been taken from our previous work.[17,18] It can be seen that the solubilities of both mandelic acid and *N*-methylephedrine are highest in the solvent (*S*)-methyl lactate, while they decrease with an increase in solvent molecule chain length from (*S*)-methyl lactate to (*S*)-butyl lactate. The effect of solvent molecule chain length on solubility has been discussed earlier on by Yalkowsky et al.[24] There, the increase in solubility with decreasing solvent molecule chain length is attributed to the well-known principle of solute−solvent interactions: "Like dissolves like".[25]

This is also true in our studies performed, which clearly shows that enantiomers of both mandelic acid and *N*-methylephedrine, which are polar molecules, dissolve better in the most polar solvent, i.e. (*S*)-methyl lactate, among the solvents studied.

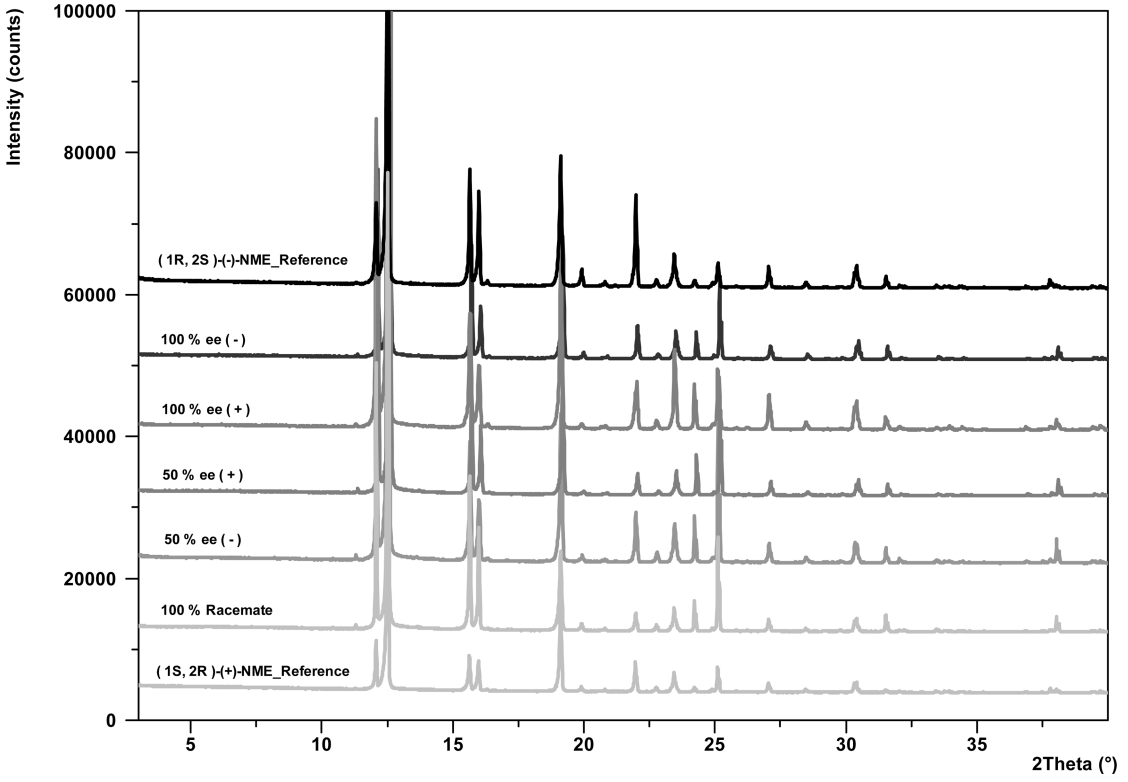

Figure 3. Experimental XRPD patterns for pure enantiomers, the racemate, and different experimental compositions of *N*-methylephedrine as found with (*S*)-butyl lactate as solvent at 25 °C (ee, enantiomeric excess).

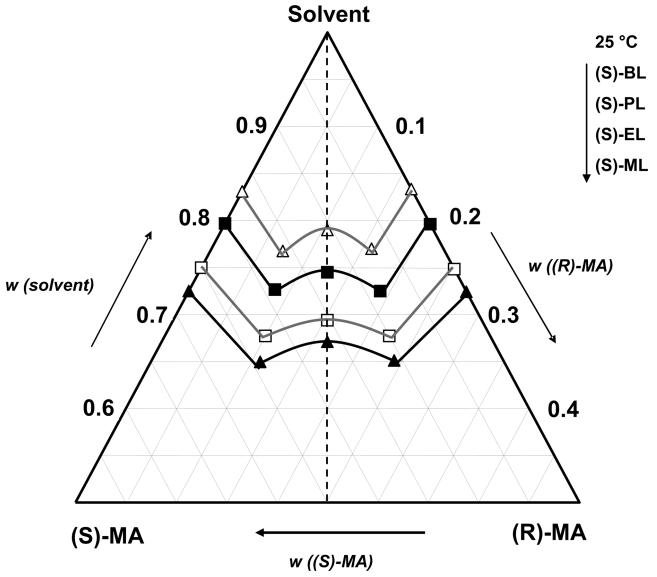

Figure 4. Solubility isotherms of mandelic acid in (*S*)-methyl lactate, (*S*)-ethyl lactate, (*S*)-propyl lactate, and (*S*)-butyl lactate at 25 °C (ML, methyl lactate; EL, ethyl lactate; PL, propyl lactate; BL, butyl lactate). The isothermal lines have been added as a visualization aid, and only the marked points show measured data.

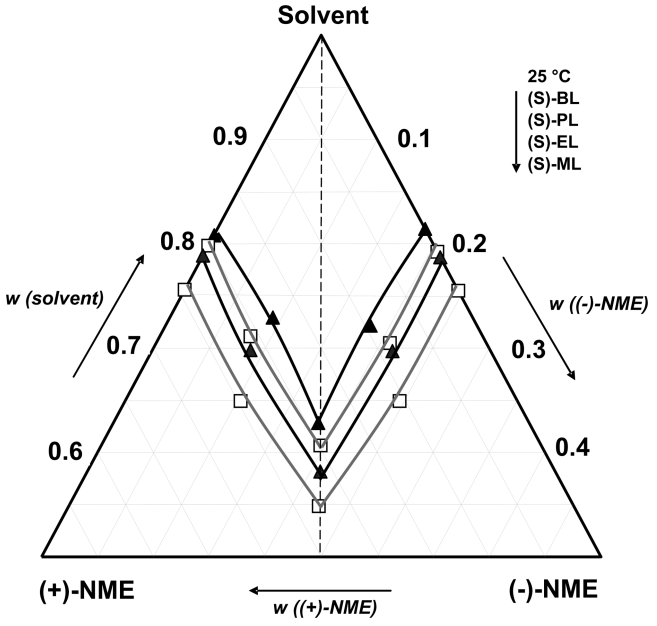

Figure 5. Solubility isotherms of *N*-methylephedrine in (*S*)-methyl lactate, (*S*)-ethyl lactate, (*S*)-propyl lactate and (*S*)-butyl lactate at 25 °C. The isothermal lines have been added as a visualization aid, and only the marked points show measured data.

Solute−Solvent Interactions in Solution for Mandelic Acid. Raman Spectra and ^{1}H NMR Measurements. Solute−solvent interactions in solution investigations were confined only to mandelic acid, since it is a compound-forming system and should be difficult to resolve. Raman spectra and ^{1}H NMR measurements were carried out for enantiomers of mandelic acid in all chiral solvents considered for the study. Exemplarily, Raman spectra of (*R*)- and (*S*)-mandelic acid in (*S*)-methyl lactate, (*S*)-ethyl lactate,[26] (*S*)-propyl lactate, and (*S*)-butyl lactate at the concentration 8 wt % are shown in Figure 6. Generally, no significant differences in the Raman spectra of the enantiomers of mandelic acid were observed, indicating the absence of measurable selective interactions of the chiral molecules and the chiral solvent in the liquid phase. The same applies to the ^{1}H NMR results not shown here. Thus, as already reported earlier for (*S*)-ethyl lactate,[26] the mandelic acid enantiomers in the lactates used did not show any considerable chiral recognition between solute and solvent. Hence, the results obtained verify that an increase or decrease in the chain length of the chiral solvent molecule does not have any significant influence on chiral discrimination. Compared to the solvent, the solute mandelic acid just exhibits two single peaks at 1587 and 3057 cm^{-1} in Figure 6.

Molecular Modeling Calculations. Molecular modeling calculations were performed to more deeply understand the effect of chain length of the chiral solvents and to evaluate how this affects the potential for enantioselective crystallization. Therefore, the enthalpies of formation of the dimers have been considered, and calculations on them are being performed. The stabilization enthalpy ($\Delta H_{\mathrm{form}}^{\mathrm{stabilization}}$) is derived from the enthalpy of formation of the dimer molecules ($\Delta H_{\mathrm{form}}^{\mathrm{dimer}}$) minus the enthalpy of formation of the single molecules of the solute and also solvent ($\Delta H_{\mathrm{form}}^{\mathrm{solute}} + \Delta H_{\mathrm{form}}^{\mathrm{solvent}}$). The $\Delta H_{\mathrm{form}}^{\mathrm{stabilization}}$ is derived by this means of subtracting the summation of the single molecules ($\Delta H_{\mathrm{form}}^{\mathrm{solute}} + \Delta H_{\mathrm{form}}^{\mathrm{solvent}}$) from that of the dimer molecules $\Delta H_{\mathrm{form}}^{\mathrm{dimer}}$, because it has been reported by Davey et al.[27] that mandelic acid in all other solvents except chloroform is strongly solvated. From the thermodynamic point of view, the dimer with the most negative $\Delta H_{\mathrm{form}}^{\mathrm{stabilization}}$ is supposed to be the most stable thermodynamically. Figure 7 illustrates a schematic representation of optimized molecular structures of the dimers of (a) (*S*)-mandelic acid and (*S*)-methyl lactate with the lactate part of the molecule (hydrogen interaction) and of (b) (*S*)-mandelic acid and (*S*)-methyl lactate with the carbon chain part of the molecule (hydrogen interaction), respectively.

The expected classical interaction is the one that would take place at the lactate part of the molecule, i.e. C═O···O−H at both points. This case of interaction is the one depicted in Figure 7a and should be stronger compared to the C═O···H−C and C═O···O−H illustrated in Figure 7b. The results are compiled in Table 1.

As can be seen in Table 1, the $\Delta H_{\mathrm{form}}^{\mathrm{stabilization}}$ of the (*S*)-mandelic acid and (*S*)-methyl lactate dimer with hydrogen bond interactions only at the lactate part of the molecule is more negative (−6.3 kcal/mol) compared to that of (*S*)-mandelic acid and (*S*)-methyl lactate with hydrogen bond interactions also at the carbon chain part which is less negative (−4.37 kcal/mol). This shows that interaction with the lactate part of the molecule is preferred compared to the carbon chain one. Therefore, the molecular modeling calculations support why no asymmetry was observed with the different chain lengths of the lactates, since the interactions with the carbon chain part play no role on chiral recognition. The molecular modeling calculations have revealed that the chain length has no influence on the chiral recognition, since it does not offer better interactions.

Furthermore, to explain why the increment in chain length of chiral solvents studied has resulted in lower solubilities and vice versa, molecular modeling calculations were performed between (*S*)-mandelic acid and two chiral solvents, (*S*)-methyl lactate and (*S*)-butyl lactate. Figure 8 depicts a schematic representation of the optimized molecular structures of the dimer of (a) (*S*)-mandelic acid and (*S*)-methyl lactate and of (b) (*S*)-mandelic acid and (*S*)-butyl lactate, respectively.

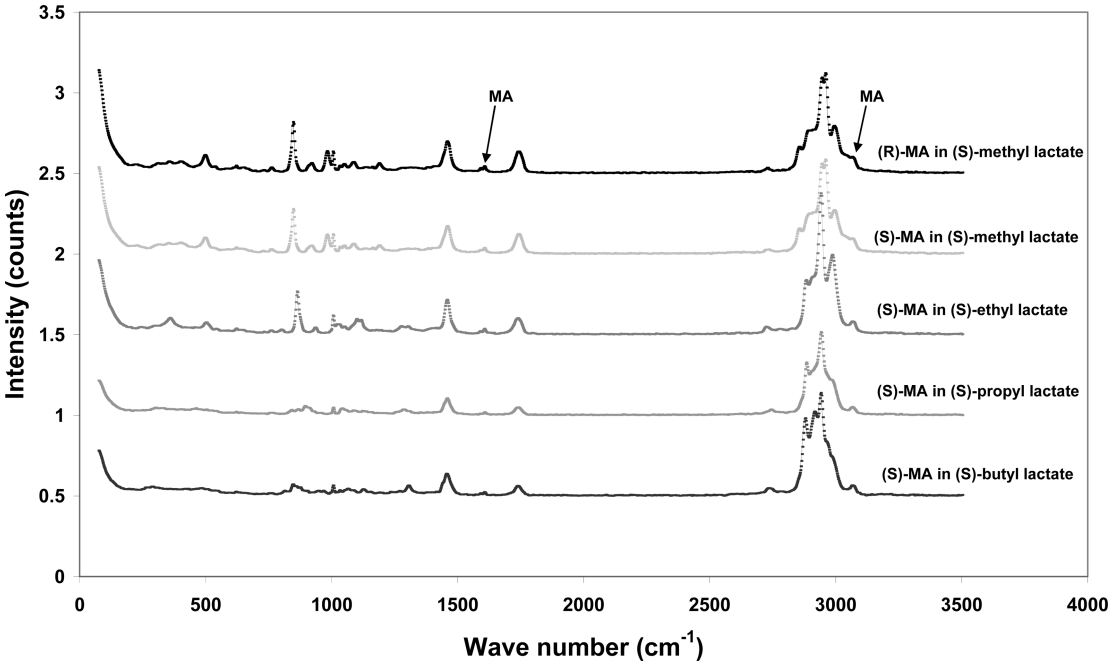

Figure 6. Exemplary Raman spectra of (*R*)- and (*S*)-mandelic acid in (*S*)-methyl lactate, (*S*)-ethyl lactate,[26] (*S*)-propyl lactate, and (*S*)-butyl lactate at a concentration of 8 wt % (MA, mandelic acid).

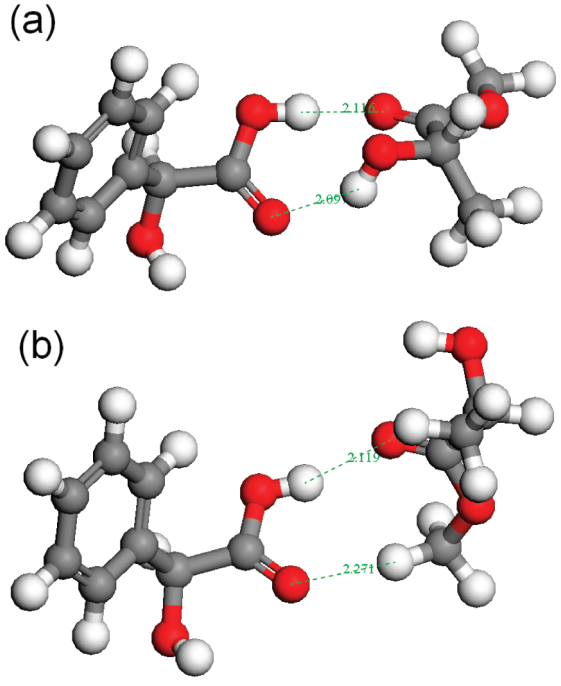

Figure 7. Schematic representation of optimized molecular structures of the dimers of (a) (*S*)-mandelic acid and (*S*)-methyl lactate with hydrogen bond interactions only at the lactate part of the molecule and of (b) (*S*)-mandelic acid and (*S*)-methyl lactate with carbon chain hydrogen interactions, respectively.

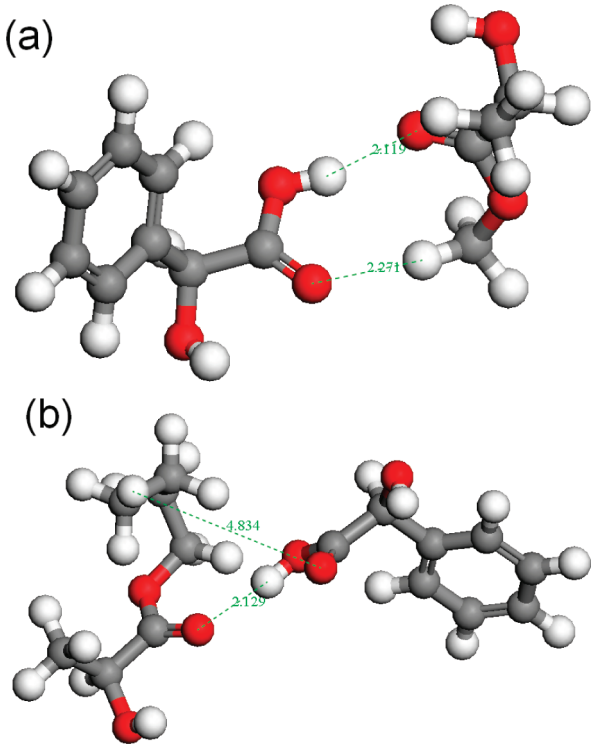

Figure 8. Schematic representation of optimized molecular structures of the dimers of (a) (*S*)-mandelic acid and (*S*)-methyl lactate and of (b) (*S*)-mandelic acid and (*S*)-butyl lactate, respectively.

Table 2 shows compilations of the enthalpies of formation of the (*S*)-mandelic acid and (*S*)-methyl lactate dimer and also the (*S*)-mandelic acid and (*S*)-butyl lactate dimer. There, it can be seen that the dimer of (*S*)-mandelic acid and (*S*)-methyl lactate has a more negative $\Delta H_{\text{form}}^{\text{stabilization}}$ value (−4.37 kcal/mol) compared to that of (*S*)-mandelic acid and (*S*)-butyl lactate, which has a less negative $\Delta H_{\text{form}}^{\text{stabilization}}$ value (−3.27 kcal/mol). Therefore, according to thermodynamics, the (*S*)-mandelic acid in (*S*)-methyl lactate dimer should be more stable, compared to the (*S*)-mandelic acid in (*S*)-butyl lactate dimer. Hence, the probability for the (*S*)-mandelic acid in (*S*)-methyl lactate dimer to be highly solvated is greater as compared to (*S*)-mandelic acid in (*S*)-butyl lactate. So, the results from the molecular modeling support why the (*S*)-methyl lactate dissolves the most compared to the other lactates studied (see Figure 5).

Table 1. Summary of Results of ΔH_{form} of Individual Molecules and Dimers of (*S*)-MA and (*S*)-Methyl Lactate (Lactate Base Hydrogen Interaction) and (*S*)-MA and (*S*)-Methyl Lactate (Carbon Chain Hydrogen Interaction)[a]

single molecule energies		dimer energies		
single molecules	$\Delta H_{form}^{solute/solvent}$ (kcal/mol)	dimer types	ΔH_{form}^{dimer} (kcal/mol)	$\Delta H_{form}^{stabilization}$ $[\Delta H_{form}^{dimer} - (\Delta H_{form}^{solute} + \Delta H_{form}^{solvent})]$ (kcal/mol)
(*S*)-MA	−117.56	(*S*)-MA−(*S*)-ML$_{lactate\ part}$	−270.00	−6.30
(*S*)-ML	−146.14	(*S*)-MA−(*S*)-ML$_{carbon\ chain}$	−268.07	−4.37

[a] MA, mandelic acid; ML, methyl lactate.

Table 2. Summary of Results of ΔH_{form} of Individual Molecules and Dimers of (*S*)-MA with (*S*)-Methyl Lactate and with (*S*)-Butyl Lactate, Respectively[a]

single molecule energies		dimer energies		
single molecules	$\Delta H_{form}^{solute/solvent}$ (kcal/mol)	dimer types	ΔH_{form}^{dimer} (kcal/mol)	$\Delta H_{form}^{stabilization}$ $[\Delta H_{form}^{dimer} - (\Delta H_{form}^{solute} + \Delta H_{form}^{solvent})]$ (kcal/mol)
(*S*)-MA	−117.56			
(*S*)-ML	−146.14	(*S*)-MA−(*S*)-ML	−268.07	−4.37
(*S*)-BL	−164.17	(*S*)-MA−(*S*)-BL	−285.00	−3.27

[a] MA, mandelic acid; ML, methyl lactate; BL, butyl lactate.

Table 3. Summary of the α_{mol}-Values of *N*-Methylephedrine in Different Chiral Solvents at 25 °C

chiral solvents	(*S*)-methyl lactate	(*S*)-ethyl lactate	(*S*)-propyl lactate	(*S*)-butyl lactate
α_{mol}-values	2.05	2.14	2.06	2.07

Relative Solubility Ratios (α_{mol} Values) of *N*-Methylephedrine. The role of the shape of the solubility isotherms and their subsequent metastable solubility lines for preferential crystallization experiments have comprehensively been discussed in the literature for conglomerate systems.[7,28,29] For conglomerates, the slope of the solubility isotherms of the enantiomers and hence the corresponding metastable solubility lines can be described with the aid of the α_{mol} value, which is defined as the ratio of the solubility of a racemic mixture to that of single enantiomers (both in mole fractions).[28] Theoretically, the crystallization trajectories of a seeded preferential crystallization process are extended for lower α_{mol} values, and a high amount of the preferred enantiomer can be crystallized and harvested, under the condition that no nucleation of the undesired counterenantiomer takes place. Thus, α_{mol} values can effectively be implemented in designing a preferential crystallization process, as they depict the shape/slope of the metastable solubility isotherms.

In the following are discussed derived α_{mol}-values for *N*-methylephedrine in the different chiral solvents in relation to ideal behavior. Table 3 contains the calculated α_{mol}-values for *N*-methylephedrine in different chiral solvents at 25 °C.

All derived α_{mol} values for *N*-methylephedrine in all solvents are close to 2. Hence, there is no effect of the chain length of the chiral solvent molecules on the solubility ratio, just on the absolute solubility values. According to the "double solubility" rule by Meyerhoffer,[30] an ideal system always shows α_{mol}-values equal to 2. However, it is important to note that this rule is applicable only in one direction.[18] If the system behaves ideally, the α_{mol}-value must be equal to 2, but when the α_{mol} value is equal to 2, the system must not necessarily be ideal. Kaemmerer et al.[18] recently reported that although *N*-methylephedrine in (*S*)-ethyl lactate has α_{mol}-values close to 2, there still exists a clear deviation from ideal behavior for this system.

Conclusions

We determined the ternary solubility phase diagrams of the compound-forming system mandelic acid and a conglomerate-forming system, *N*-methylephedrine, in chiral solvents, (*S*)-methyl lactate, (*S*)-propyl lactate, and (*S*)-butyl lactate. The measured ternary solubility phase diagrams for both chiral systems showed symmetric behavior. This clearly indicates that the chain length of the chiral solvents investigated in this work had no measurable enantioselective influence on the solution thermodynamics of the chiral systems mandelic acid and *N*-methylephedrine. Even though the absolute solubility value differs, no effect on the solubility ratio was observed. Molecular modeling calculations could support the experimental results. However, *N*-methylephedrine showed deviation from the ideal behavior, although the calculated α_{mol} values for *N*-methylephedrine were close to 2.

Taking into consideration the requirements of crystallization based enantioseparation processes, the effects of temperature and solvent molecule chain length on the shapes of solubility isotherms and the α_{mol} values were studied.

Acknowledgment. The authors thank Ir. Gert L. Nanninga of Purac Company, The Netherlands, for providing the chiral solvents. Also, the authors thank J. Kaufmann and L. Borchert at Max Planck Institute in Magdeburg for help with experimental work and L. Hilfert at Otto-von-Guericke University, Magdeburg, for conducting ^{1}H NMR measurements.

References

(1) Millership, J. S.; Fitzpatrick, A. *Chirality* **1993**, *5*, 573–576.
(2) Stinson, S. C. *Chem. Eng. News* **1997**, *75*, 38–70.
(3) McConathy, J.; Owens, M. J. *J. Clin. Psychiatry* **2003**, *5*, 70–73.
(4) Maier, N. M.; Franco, P.; Lindner, W. *J. Chromatogr., A* **2001**, *906*, 3–33.
(5) Pasteur, L. *Ann. Chim. Phys.* **1848**, *3*, 442–459.
(6) Roozeboom, H. W. B. *Z. Phys. Chem.* **1899**, *28*, 494–517.
(7) Collet, A.; Brienne, M. J.; Jacques *J. Chem. Rev.* **1980**, *80*, 215.
(8) Collet, A. *Enantiomer* **1999**, *4*, 157–172.
(9) Collins, A. N., Sheldrake, G. N., Crosby, J., Eds. *Chirality in Industry: The Commercial Manufacture and Applications of Optically Active Compounds*; Wiley & Sons: Chichester, 1992.
(10) Collins, A. N., Sheldrake, G. N., Crosby, J., Eds. *Chirality in Industry II: Developments in the Manufacture and Applications of Optically Active Compounds*; Wiley & Sons: Chichester, 1997.
(11) Kostova, A.; Bart, H. *Sep. Purif. Technol.* **2007**, *54*, 340–348.
(12) Sakai, K.; Yokoyama, M.; Sakurai, R.; Hirayama, N. *Tetrahedron: Asymmetry* **2006**, *17*, 1541–1543.
(13) Lorenz, H.; Polenske, D.; Seidel-Morgenstern, A. *Chirality* **2006**, *18*, 828–840.
(14) Francisca, R.; Ramón, L. *J. Chem. Educ.* **2005**, *82*, 930.
(15) Coquerel, G. *Top. Curr. Chem.* **2007**, *269*, 1–51.
(16) Myerson, A. S. *Handbook of Industrial Crystallization*; Butterworth-Heinemann: Oxford, 2002.
(17) Tulashie, S. K.; Kaemmerer, H.; Heike, L.; Seidel-Morgenstern, A. *J. Chem. Eng. Data* **2010**, *55*, 333–340.

(18) Kaemmerer, H.; Tulashie, S. K.; Heike, L.; Seidel-Morgenstern, A. *J. Chem. Eng. Data* **2010**, *55*, 1131–1136.
(19) Accelrys Software Inc. *Materials Studio Release Notes, Release 4.3*; Accelrys Software Inc.: San Diego, 2008.
(20) Goodman, J. M. *Chemical applications of molecular modelling*; The Royal Society of Chemistry: Cambridge, 1998.
(21) Hinchliffe, A. *Molecular Modelling for Beginners*, 2nd ed.; John Wiley & Sons Ltd: Chichester, 2008.
(22) Lorenz, H.; Seidel-Morgenstern, A. *Thermochim. Acta* **2004**, *415*, 55–61.
(23) Lorenz, H.; Sapoundjiev, D.; Seidel-Morgenstern, A. *J. Chem. Eng. Data* **2002**, *47*, 1280–1284.
(24) Yalkowsky, S. H.; Flynn, G. L.; Slunick, T. G. *J. Pharm. Sci.* **1972**, *61*, 852–857.
(25) Reichardt, C. *Solvents and Solvent Effects in Organic Chemistry*; Wiley−VCH: Weinheim, Germany, 2003.
(26) Tulashie, S. K.; Heike, L.; Liane, H.; Edelmann, F. T.; Seidel-Morgenstern, A. *Cryst. Growth Des.* **2008**, *8*, 3408–3414.
(27) Davey, R. J.; Dent, G.; Mughal, R. K.; Parveen, S. *Cryst Growth Des.* **2006**, *6*, 1788–1796.
(28) Jacques, J.; Collet, A.; Wilen, S. H. *Enantiomers, Racemates and Resolutions*; Krieger Publishing Company: Malabar, FL, 1994.
(29) Levilain, G.; Tauvel, G.; Coquerel, G. How homogenous equilibria between solvated enantiomers can modify the stable and metastable heterogeneous equilibria, *Proc. 13th BIWIC*; Jansens, J. P., ter Horst, J. H., Jiang, S., Eds.; IOS Press: Delft, The Netherlands, 2006; pp 244−250.
(30) Meyerhoffer, W. *Ber. Dtsch. Chem. Ges.* **1904**, *37*, 2604–2610.